Supporting Information

Structural changes in $HfSe_2$ and $ZrSe_2$ thin films with various oxidation methods

Alexandre C. Foucher[1], Wouter Mortelmans, [1] Bing Wu,[2] Zdenek Sofer,[2] Rafael Jaramillo [1], Frances M. Ross[1,*]

[1] Department of Materials Science and Engineering, Massachusetts Institute of Technology, Cambridge, Massachusetts 02139, United States

[2] Department of Inorganic Chemistry, University of Chemistry and Technology Prague, Technická 5, 166 28 Prague 6, Czech Republic

*Corresponding author: fmross@mit.edu

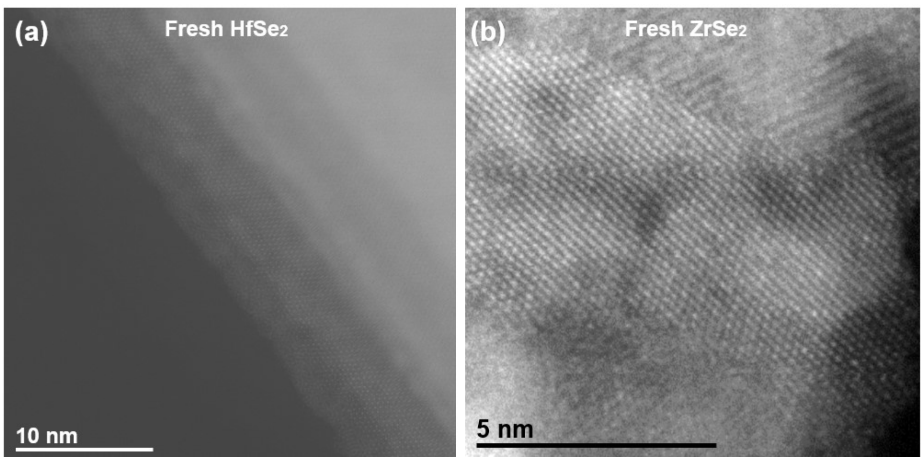

Figure S1. STEM images of freshly exfoliated samples to show other regions of (a) $HfSe_2$; (b) $ZrSe_2$.

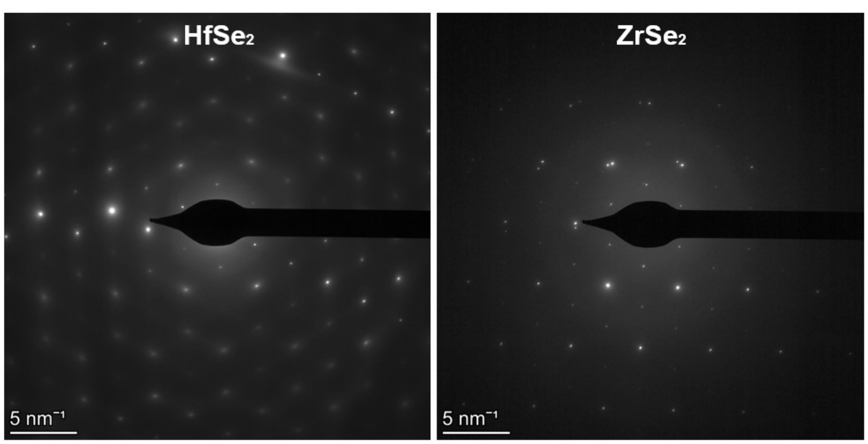

Figure S2. Diffraction pattern along [001] zone axis, perpendicular to the surface of the flakes. The sample was slightly tilted in $HfSe_2$. For $ZrSe_2$, there were two overlapping crystals, explaining the double spots. The diffraction patterns are consistent with symmetries found in $P\bar{3}m1$.

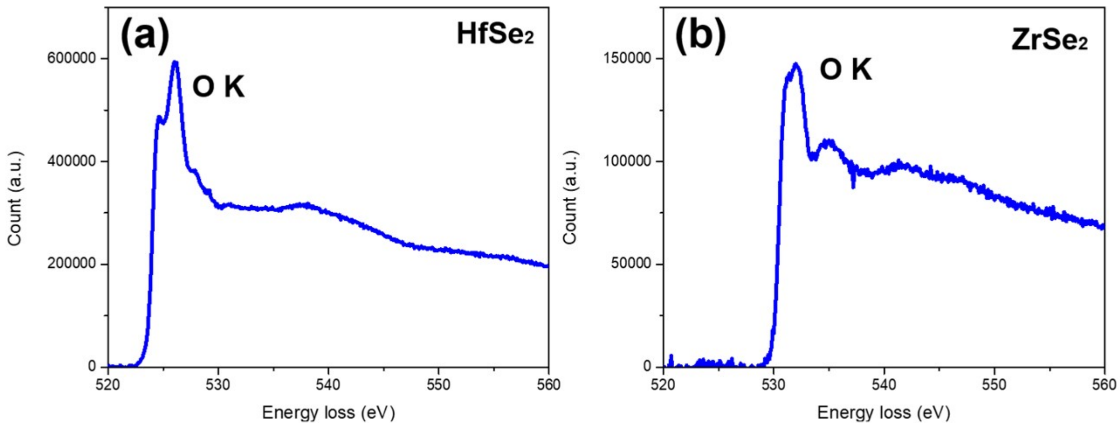

Figure S3. EELS data of the O K edge for the two materials after oxidation in air at room temperature. The shape of the edge is consistent with an oxidation state of +IV for both metals. (a) $HfSe_2$. (b) $ZrSe_2$.

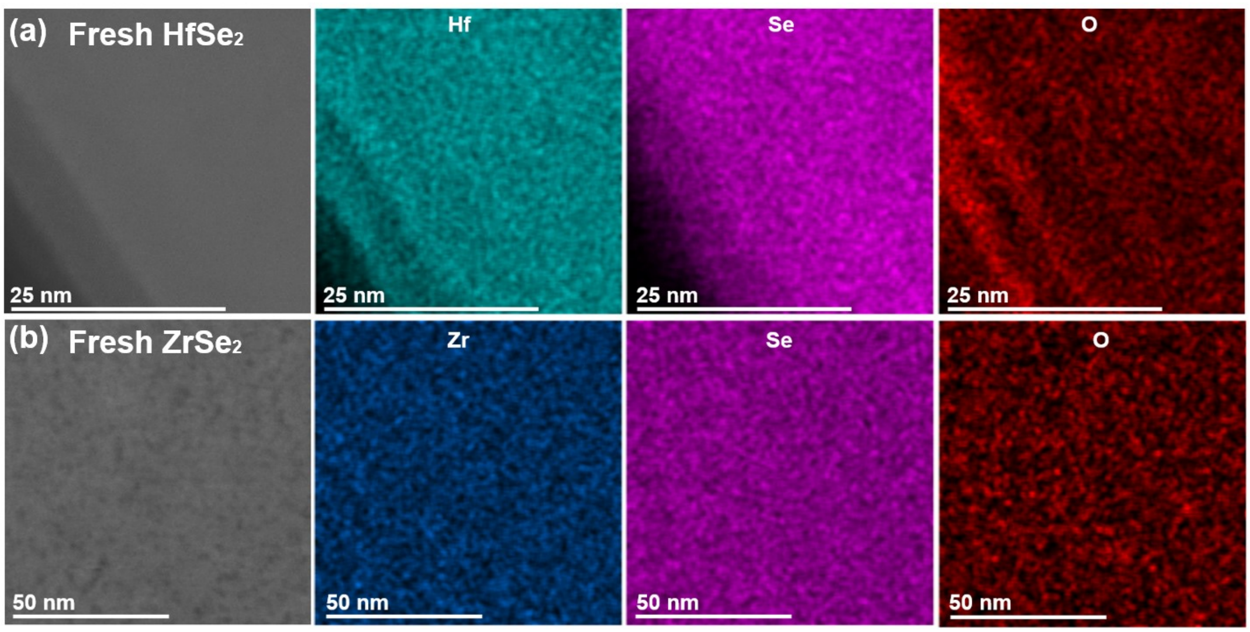

Figure S4. EDS analysis of freshly exfoliated (a) $HfSe_2$ and (b) $ZrSe_2$. No segregation of Se is visible in the fresh samples.

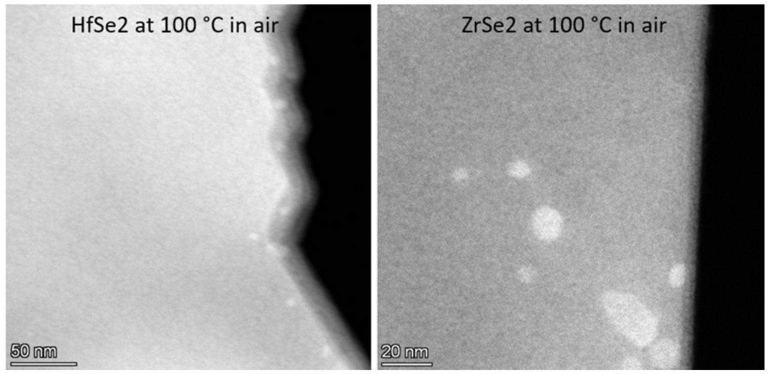

Figure S5. Flakes after oxidation in air at 100 °C for 20 minutes. Segregation of Se was observed, as for flakes oxidized in air at room temperature.

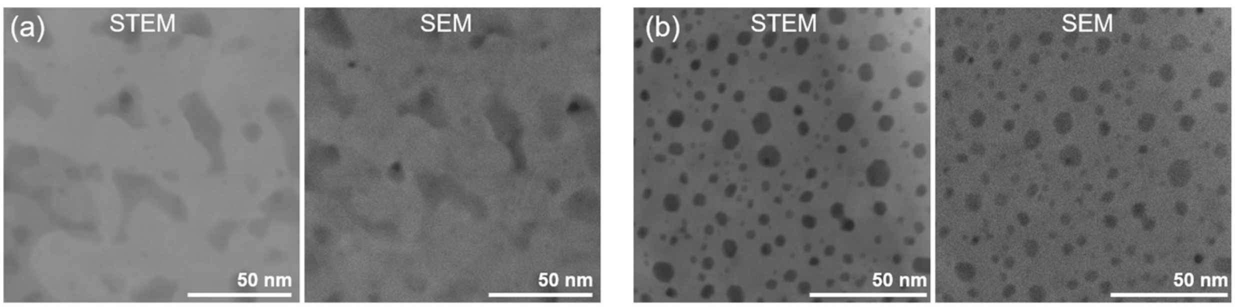

Figure S6. Simultaneously acquired STEM and SEM images showing pits at the surface of (a) $HfSe_2$ and (b) $ZrSe_2$ after heating. Many cavities appear to be at the surface.

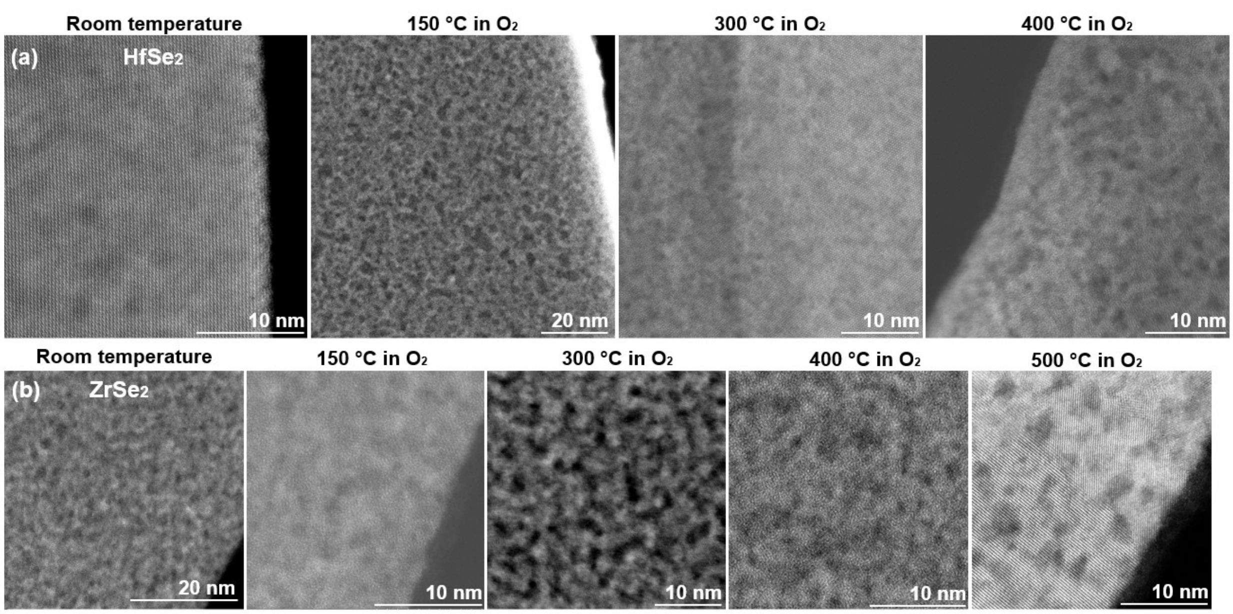

Figure S7. Heating of (a) $HfSe_2$ flake and (b) $ZrSe_2$ flake with *in situ* STEM at 10 Pa of O_2. Defects can be seen at the indicated temperature, showing that thermal oxidation is not an ideal method.

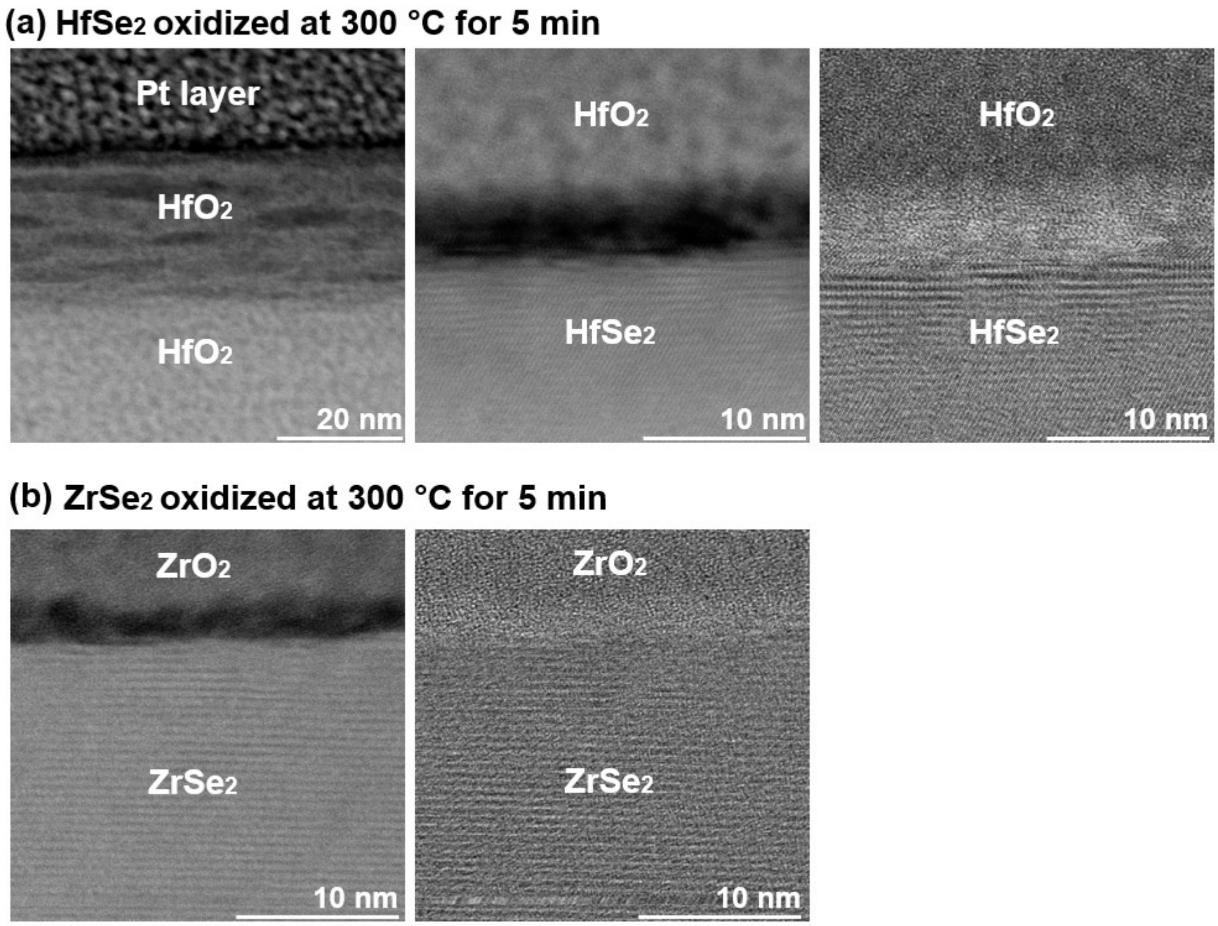

Figure S8. Cross-sections of samples heated in air (1bar) at 300 °C in a furnace for 5 minutes. (a) $HfSe_2$ oxidized into HfO_2, with defects in HfO_2 and delamination between the oxide and $HfSe_2$. (b) Delamination of the ZrO_2 layer on top of $ZrSe_2$. The results underline that thermal oxidation at 1 bar is not an efficient method.

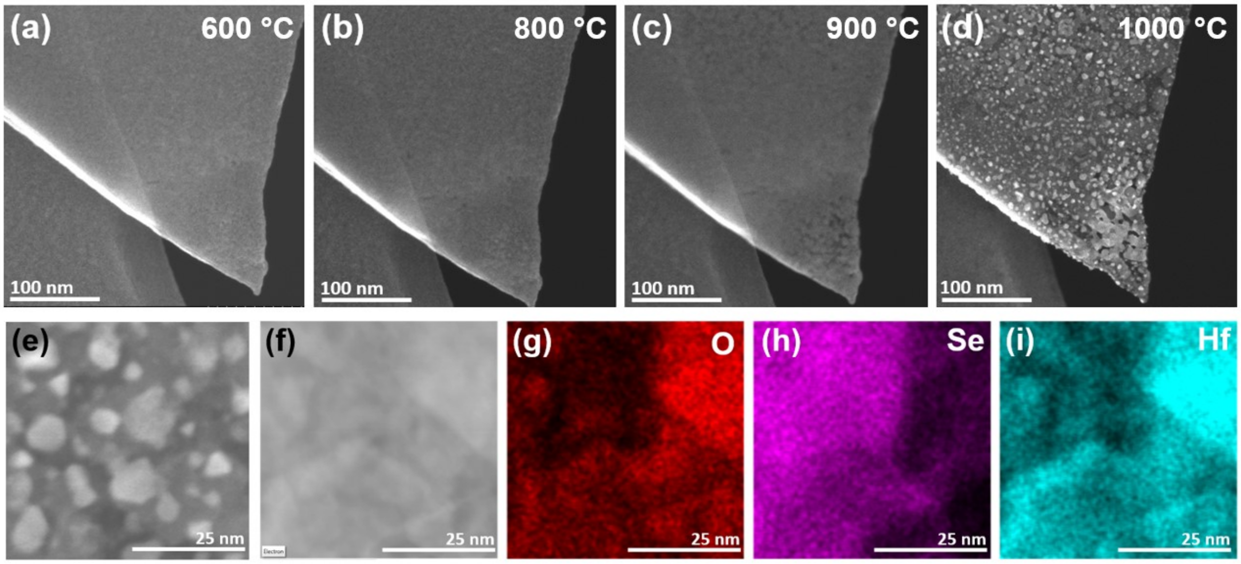

Figure S9. Structural changes on heating under vacuum of an $HfSe_2$ flake. (a-d) SEM images showing $HfSe_2$ flake after heating to the temperatures indicated. Islands are visible at temperatures above 900 °C. (e) SEM image showing islands on the surface after the sample was cooled down in vacuum. (f) Corresponding HAADF-STEM image. (g-i) Corresponding EDS maps for O, Se and Hf showing that the sample remains oxidized even after annealing in vacuum at 1000 °C.

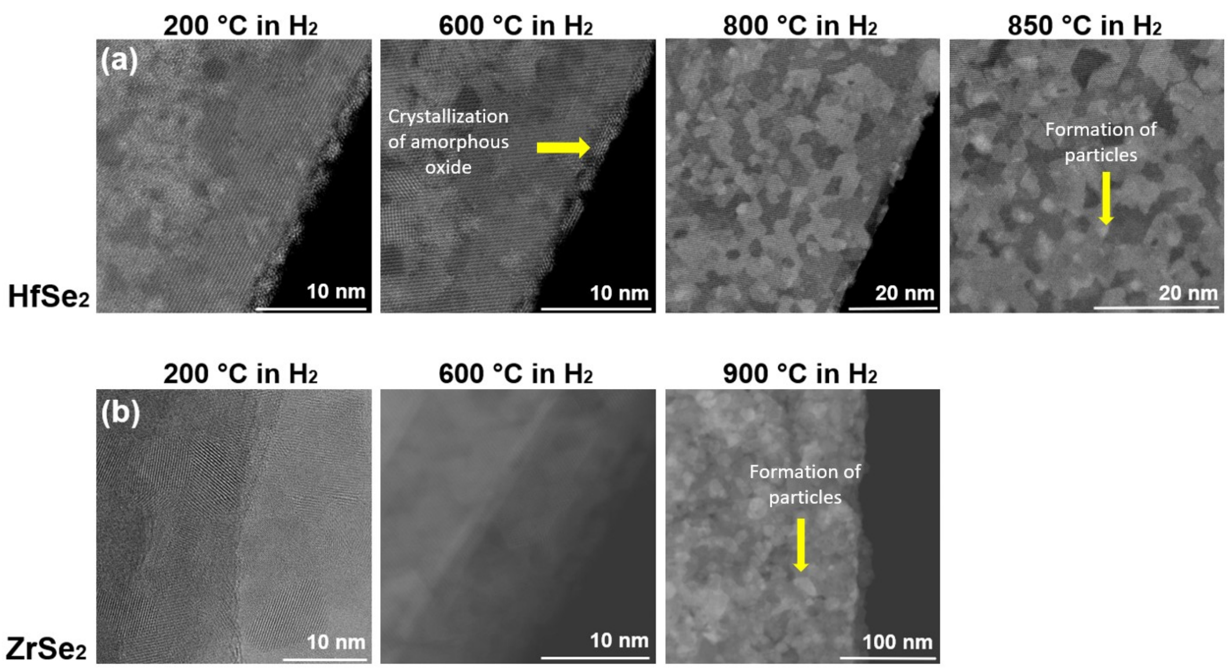

Figure S10. Progressive reduction of the materials showing changes in configuration and formation of sharp interfaces and islands. (a) Reduction under H_2 of $HfSe_2$. (b) Reduction under H_2 of $ZrSe_2$.

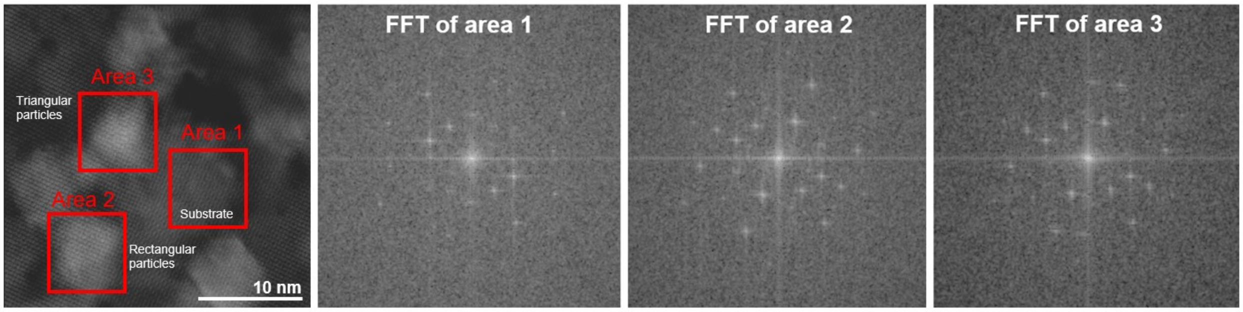

Figure S11. Analysis of HAADF-STEM image of $ZrSe_2$ after reduction. FFT analysis of underlying flake (area 1) suggests epitaxy with the islands, either rectangular (area 2) or triangular (area 3).

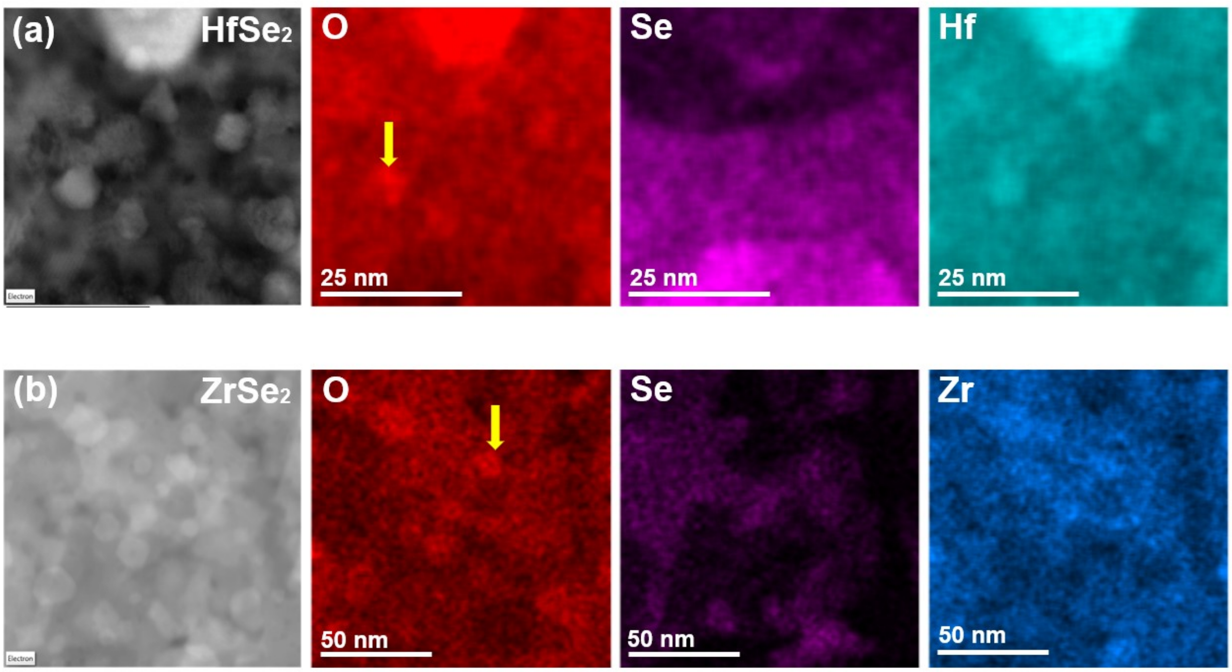

Figure S12. EDS analysis of $HfSe_2$ and $ZrSe_2$ flakes after exposure to H_2 for 1 hour at 1050 °C. (a) HAADF-STEM image of $HfSe_2$, and corresponding EDS maps for O, Se, and Hf. The islands show a strong signal for Hf and O (yellow arrow), suggesting that Hf oxides form a substantial part of the structure. (b) HAADF-STEM image of $ZrSe_2$, and corresponding EDS maps for O, Se, and Zr. The islands show a strong signal for Zr and O (yellow arrow) similar to the result for $HfSe_2$.

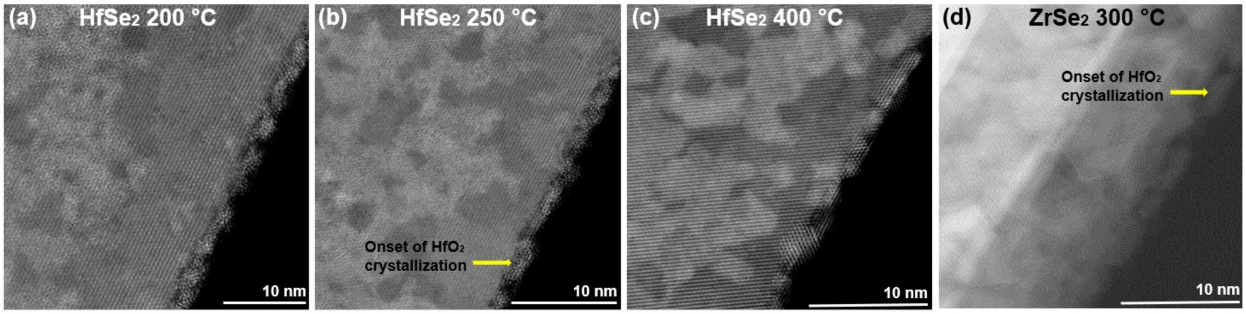

Figure S13. Annealing in H_2 shows the progressive crystallization of amorphous oxide detected in fresh samples. (a-c) Annealing of $HfSe_2$, showing the transition of amorphous to a crystalline phase starting at 250 °C. (d) Annealing of $ZrSe_2$ causes crystallization at 300 °C.

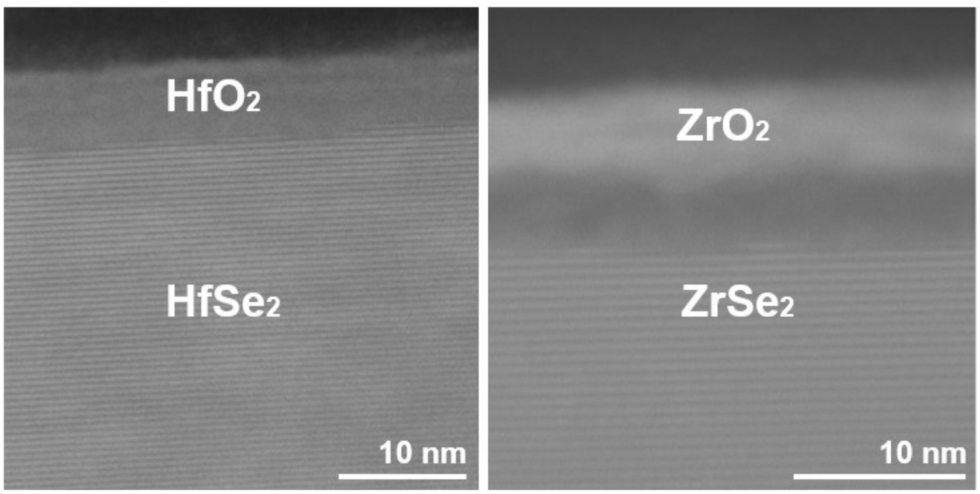

Figure S14. Additional images of the cross section of plasma-oxidized flakes. Some delamination can sometimes be observed, as seen by the small gap between the ZrO_2 layer and the $ZrSe_2$ structure.

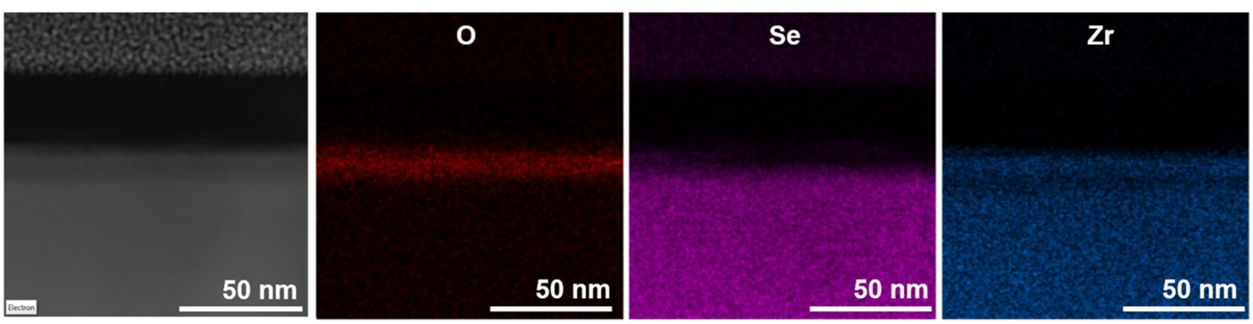

Figure S15. Cross sectional imaging of $ZrSe_2$ after plasma oxidation. The corresponding EDS maps show a uniform distribution of O, Se and Hf. Delamination of the ZrO_2 oxide layer can be seen on the EDS map of Zr.